Reaction Chemistry & Engineering

ROYAL SOCIETY OF CHEMISTRY

PAPER

View Article Online
View Journal

Cite this: DOI: 10.1039/d6re00082g

Studying deactivation pathways of molecular catalysts *ex situ*: an accessible method using standard analytical equipment

Lisa Steinwachs, Sven Störtte, Peter McNeice and Andreas J. Vorholt *

Received 10th March 2026,
Accepted 31st March 2026

DOI: 10.1039/d6re00082g

rsc.li/reaction-engineering

In this contribution we propose a new *ex situ* method to monitor catalyst stability during continuous reactions as an alternative to *operando* spectroscopy. This is achieved by analyzing samples from the product collector of a continuous operated miniplant using gas chromatography, X-ray fluorescence, and mass spectrometry. Combining these standard analytical techniques allowed us to study the decomposition pathway of the molecular catalyst that was the degradation of the ligand *via* alkyl/aryl exchange. This new method will allow accessible, real-time monitoring of catalyst stability. In future this method can be used to adjust reaction conditions on the fly to maintain the lifetime and performance of the catalyst system.

Introduction

Continuous monitoring of catalyst stability is a pressing concern in reaction engineering.[1–5] This is true for both developing new catalysts and performing established reactions. For both homogeneous and heterogeneous catalysts, altering the reaction conditions in real-time can maintain product selectivity and catalyst lifetime. Currently, real-time monitoring of catalyst systems is performed by *operando* spectroscopic techniques.[1,6–9]

In homogeneous catalysis, *operando* spectroscopy has mainly been applied to explore reaction mechanisms and reaction kinetics,[10–12] but more recently it has also been used for investigations into catalyst deactivation.[6,13–15] This information can be used to improve catalyst lifetime by adjusting reaction conditions. For example, during the methoxycarbonylation of ethylene, the decomposition of the palladium catalyst could be monitored and prevented by manual dosing of TsOH and PPh_3 during the reaction.[16] The mechanism of decomposition was determined using *operando* NMR which showed the formation of a phosphonium ion from the PPh_3 ligand. Despite major breakthroughs in *operando* analysis for monitoring catalytic reactions to assess and prevent catalytic deactivation,[6,13,14,16] the topic of deactivation of molecular catalysts is a very under-exposed field of research. A limitation is that *operando* spectroscopy requires specialist equipment which is not readily available to many research groups. This limitation is also reflected in the literature on catalyst deactivation, where a survey by Martín *et al.* revealed that only 3% of studies employed *in situ* or *operando* analytical techniques, highlighting the continued reliance on *ex situ* methods for investigating catalyst deactivation.[2] For example, a deactivation study by Vossen *et al.* demonstrated the degradation of the phosphorus ligand biphephos in the presence of oxygen and water using *ex situ* analytical techniques such as NMR spectroscopy and atmospheric pressure chemical ionization mass spectrometry (APCI-MS).[17]

Additionally, the study of molecular catalyst deactivation is complicated by the requirement for efficient recycling of homogeneous catalysts. Strategies for homogeneous catalyst recycling and reaction metrics that can be used to monitor catalyst stability have been discussed in a recent review.[18] Using hydroformylation as an example, as in the present study, the authors state that a reduction in selectivity can provide information on ligand degradation, as a decrease in selectivity may indicate ligand loss or decomposition. However, since selectivity can be influenced by both factors, it is not possible – without the use of operando analytical techniques – to directly attribute an observed decrease in selectivity to ligand deactivation.

A method is missing in literature to directly correlate a decrease in selectivity with ligand deactivation by methods which don't have to use specialized inline spectroscopic equipment. To develop this method, a process is required in which the recycling concept is designed such that deactivated ligand species preferentially leave the system. For such a process, the extent of ligand deactivation can be derived both from the observed selectivity and from the amount of leaching determined by analysis of the product stream, without the need for operando equipment (Fig. 1).

Max Planck Institute for Chemical Energy Conversion, Stiftstraße 34-36, 45470 Mülheim an der Ruhr, Germany. E-mail: Andreas-j.vorholt@cec.mpg.de

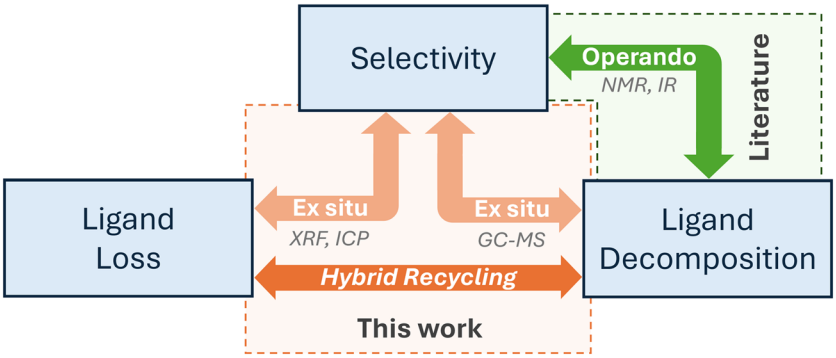

Fig. 1 Correlation between selectivity, ligand loss, and ligand degradation during continuous operation for a process without a dedicated hybrid recycling concept and a process with a hybrid recycling concept.

To develop a recycling concept that meets these requirements, liquid–liquid multiphase recycling for a hydroformylation/aldol-condensation tandem reaction was complemented by membrane separation. Both recycling strategies had previously been investigated in our group using a rhodium-sulfoxantphos catalyst.[19] In these studies, no correlation between changes in selectivity and ligand decomposition was observed for either method. Integrating these two approaches into a hybrid recycling technique offers substantial potential to enhance catalyst recycling efficiency and to enable process intensification.[20–22] Using this advanced recycling concept, we demonstrate that the detailed analysis of the product phase can give deep insights into the fate of the molecular catalyst. With a combination of X-ray fluorescence (XRF), gas chromatography (GC-FID) and mass spectrometry we observed decomposition of the sulfoxantphos ligand, alongside a corresponding drop in catalyst selectivity.

Results

We validated the proposed *ex situ* method for monitoring ligand decomposition using a tandem reaction consisting of the hydroformylation of 1-hexene catalysed by a rhodium-sulfoxantphos complex, followed by a base-catalysed aldol condensation (Fig. 2). This system uses a polar ligand that is soluble in the polar solvent PEG200. The aldol-products form a second liquid phase that contains a fraction of ligand and metal.[23,24]

The reaction was carried out in a miniplant equipped with a closed recycle loop (Fig. 3). The miniplant consists of a 300 mL continuous stirred window-reactor (CSTR) which was temperature-controlled using a heating mantle, a decanter, and the membrane unit. At the start of the reaction, both the hydroformylation catalyst and the aldol condensation catalyst were dissolved in PEG200 and subsequently charged into the reactor. In addition, the substrate 1-hexene was continuously fed to both the reactor and the decanter. Initially, the reaction was operated for 10 hours in semi-batch mode under continuous gas supply, with the valve to the membrane loop closed and only the circulation between the reactor and the decanter in operation. As the formation of the C14 aldol products progressed, the organic phase became increasingly nonpolar, resulting in the formation of a biphasic system in the decanter consisting of a polar catalyst-rich phase and an organic product phase. After 10 hours, continuous operation was initiated, at which point the membrane loop with a BORSIG oNF-2 (ref. 25) membrane was also brought into operation. The organic product phase was withdrawn from the decanter *via* a dip tube and pumped to the membrane unit, while the polar catalyst phase was returned from the bottom of the decanter to the reactor. The permeate was collected in a product vessel.

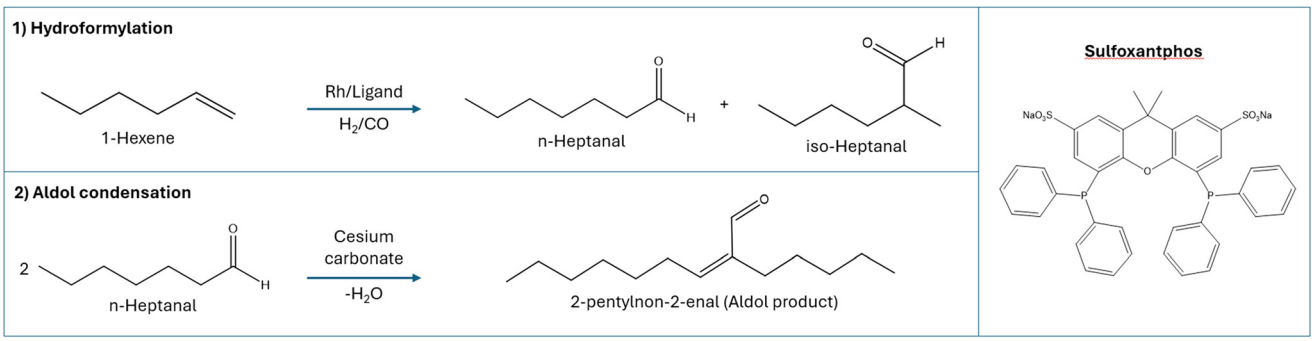

Fig. 2 The hydroformylation of 1-hexene catalyzed by our rhodium/ligand system and the aldol condensation of the heptanal catalyzed by cesium carbonate and the structure of the ligand sulfoxantphos.

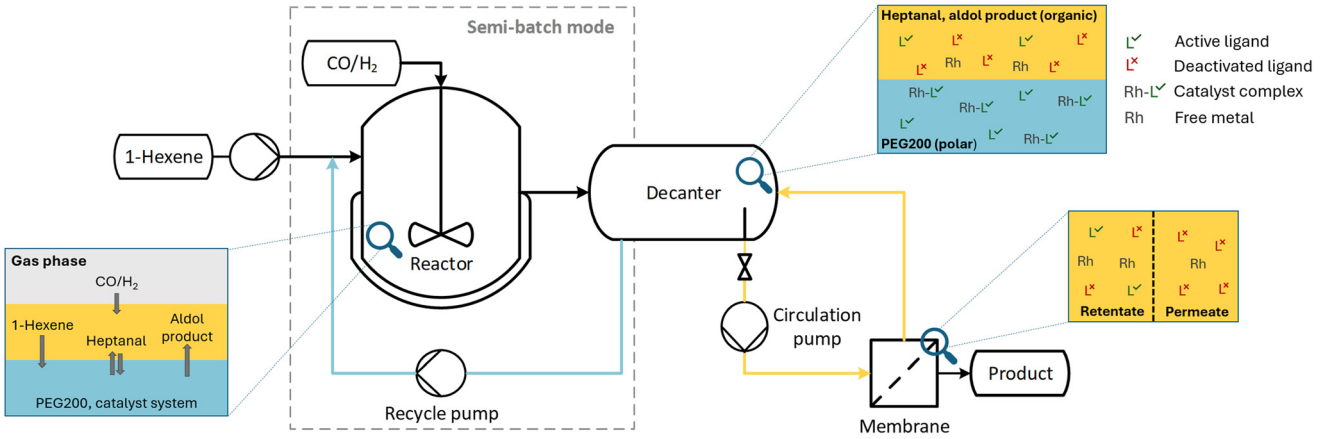

Fig. 3 The miniplant set-up used for the continuous tandem reaction.

Due to the polar nature of the sulfonic acid group of sulfoxantphos, the rhodium–ligand complex as well as the free, active ligand exhibits a higher solubility in the polar solvent PEG-200 than in the organic phase. If one of the phosphorus atoms is no longer bound to the sulfonic acid group as a result of deactivation, it can be assumed that the detached phosphorus-containing species preferentially partitions into the organic product phase. Such ligand deactivation therefore results in increased phosphorus leaching into the organic phase. However, since PEG-200 is partially miscible with the organic phase, the solubility of the active ligand in the organic phase is not zero. In a previous continuous experiment employing this reaction system and the multiphasic recycling approach, a rhodium content of 4–12 ppm was detected in the organic phase.[19] Consequently, the extent of ligand deactivation cannot be determined solely on the basis of phosphorus leaching.

To prevent loss of the active ligand from the system *via* the organic phase, the organic stream was additionally passed through a membrane unit, which in a preceding continuous recycling experiment with this reaction system exhibited a rhodium concentration of only 0.1 ppm in the permeate.[19] It is often reported that a range of linked factors affect membrane retention. Physico-chemical interactions between solute and solvent, solvent and membrane, and solute and membrane can be the dominant reason for separation.[26–31] Previous studies from our group with various phosphorus-containing ligands have demonstrated that the high ligand retention of the membrane originates from the charge of the sulfonic acid group (see SI, Section 1). Once this group is no longer present, *i.e.* when the ligand is deactivated, phosphorus retention decreases significantly. Integration of the membrane into the process therefore ensures that only deactivated ligand species are removed from the system.

The continuous reaction was operated for a total duration of 43 hours. At the beginning, a decrease in 1-hexene conversion from 94% to 90% is observed within the first 3.5 hours (Fig. 4). During the 10 hour semi-batch phase, a high conversion is achieved in the system, leading to a strong increase in product concentration in the reaction solution. Under continuous operation, this reaction solution is gradually washed out. Because the high conversion attained during the 10 hour semi-batch phase cannot be maintained at the residence time of 7 hours applied during continuous operation, the product concentration in the system decreases, and consequently the measured conversion drops immediately after the semi-batch phase. Subsequently, the conversion remains stable at a level above 90% until hour 20. The yield of the aldol products remains stable during the first 6.5 hours and subsequently decreases until the end of the experiment. A similar decline has been reported previously for this system and can be attributed to the progressive accumulation of water, which is formed as a byproduct of the aldol condensation.[19,23,32] The increasing water content in the polar phase reduces the basicity of the aldol condensation catalyst (see SI, Section 2), which is presumably responsible for the observed decrease in reaction

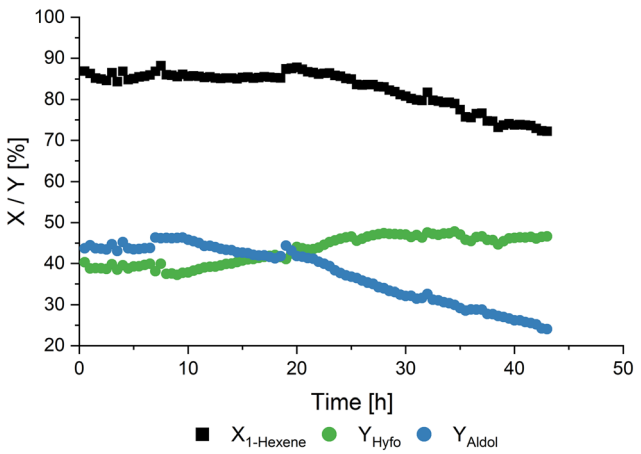

Fig. 4 The hexene conversion and yield of the hydroformylation and aldol condensation products during the continuous reaction. Reaction conditions: T = 125 °C, p = 50 bar, $x_{Rh/P}$ = 1 : 4, $n_{[Rh(acac)(CO)_2]}$ = 0.3 mol%, $n_{Sulfoxantphos}$ = 0.6 mol%, $n_{Cs_2CO_3}$ = 7.5 mol%, $n_{(CO)}$ = $n_{(H_2)}$ = 1 mol h^{-1}, $V_{(Hexene)}$ = 16 mL h^{-1}, $V_{Recycle}$ = 200 mL h^{-1}, $m_{(Circulation)}$ = 60 kg h^{-1}.

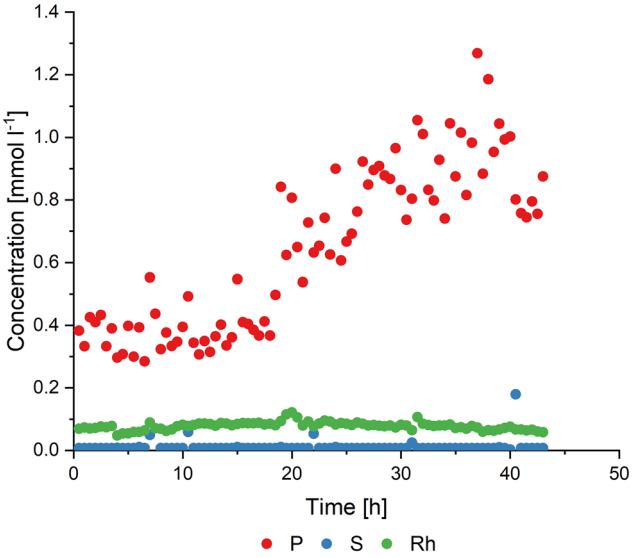

Fig. 5 The concentration of phosphorous, sulfur and rhodium in the permeate stream. Reaction conditions: T = 125 °C, p = 50 bar, $x_{Rh/P}$ = 1 : 4, $n_{[Rh(acac)(CO)_2]}$ = 0.3 mol%, $n_{Sulfoxantphos}$ = 0.6 mol%, $n_{Cs_2CO_3}$ = 7.5 mol%, $n_{(CO)} = n_{(H_2)}$ = 1 mol h^{-1}, $V_{(Hexene)}$ = 16 mL h^{-1}, $V_{Recycle}$ = 200 mL h^{-1}, $m_{(Circulation)}$ = 60 kg h^{-1}.

activity. Since the aldol condensation consumes the hydroformylation products as reactants, a decline in aldol activity directly results in an increased yield of hydroformylation products. After 20 hours, the overall conversion steadily declines, reaching 83% after the total operating time of 43 hours. This decrease indicates a gradual loss of hydroformylation activity.

GC-FID was used to analyze the *n*/iso selectivity, while XRF was employed to quantify the leaching of phosphorus, sulfur and rhodium.

The rhodium concentration in the permeate stream of the membrane separation unit remained approximately constant over the entire duration of the continuous experiment, with an average value of 0.078 mmol l^{-1} (Fig. 5). During the first 12.5 hours of operation, phosphorus leaching remained constant as well, with an average concentration of 0.44 mmol l^{-1} in the permeate stream. After 12.5 hours, the phosphorus concentration began to increase steadily, reaching a value of 0.94 mmol l^{-1}, corresponding to a total phosphorus loss of 22.8% after 43 hours. However, with an average of 0.03 mmol l^{-1} only minimal levels of sulfur were detected in the product collector. This observation indicates that ligand decomposition is occurring, with a phosphine moiety passing through the membrane, while a sulfate-containing fragment remains in the reactor loop. This behavior cannot be resolved by XRF analysis, which provides only concentrations of the elements and no structural information on the leached species. To gain a deeper insight into the decomposition products, mass spectrometry was therefore employed to investigate their molecular structures.

Mass spectrometric analysis revealed a signal at 286 g mol^{-1} corresponding to diphenylhexylphosphine oxide (DPHPO), as well as a signal at 215 g mol^{-1} attributed to diphenylmethylphosphine oxide (DPMPO), a known

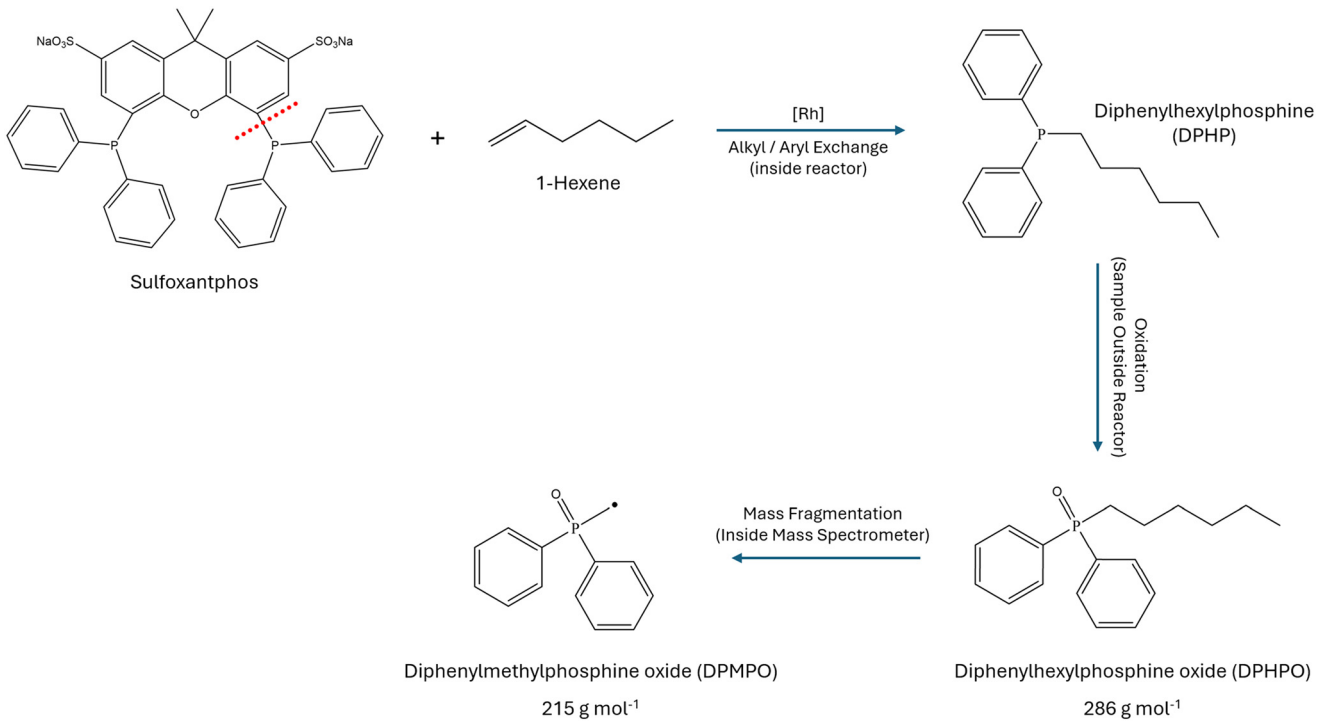

Fig. 6 Decomposition of the sulfoxantphos ligand *via* alkyl/aryl exchange, and subsequent oxidation outside the reactor, leading to a phosphine oxide moiety. The remaining ligand stays in the reactor due to retention by the membrane.

fragmentation product of the hexyl analogue (see SI, Section 3). In literature, it has been reported that under hydroformylation conditions an alkyl/aryl exchange reaction can occur.[1,33] We therefore propose that the sulfoxantphos ligand undergoes such an exchange, with the resulting diphenylhexylphosphine (DPHP) being oxidized to diphenylhexylphosphine oxide (DPHPO) outside the reactor (Fig. 6) We assume that this oxidation occurred outside the reactor, as the process was conducted under inert conditions throughout and all solvents were thoroughly degassed prior to use. This mechanism accounts for the observed phosphorus leaching while explaining the absence of sulfur detected in the product collector.

The evolution of the DPHPO peak area and the phosphorus concentration in the permeate stream show the same trend (Fig. 7). Both remain constant during the first 12.5 h, increase slightly until hour 18, and then rise sharply until the end of the experiment after 43 h. This behavior confirms that ligand deactivation is responsible for the increasing phosphorus loss and that a major fraction of the phosphorus detected in the permeate stream leaves the system in the form of the ligand degradation product DPHP.

Alongside the leaching values we observed a decrease in the *n*/iso ratio, beginning at 18 h (Fig. 8). This corresponds to the time where the phosphine leaching increased strongly. This decrease in catalyst selectivity is therefore directly linked to the ligand leaching, which occurs because of ligand degradation.[19] Aside from several anomalies, the turnover frequency (TOF) remains consistent. As the selectivity decreases, the stable TOF supports a decomposition and loss of ligand, but retention of the rhodium species.[19]

Taken together, the *n*/iso ratio and TOF (from GC), leaching data (from XRF), and leaching species (mass spectrometry) provide an insight into the catalyst decomposition. We propose analysis of the permeate solution (*ex situ*) to be a convenient alternative to *operando* measurements for monitoring catalyst stability. These analytics can be conducted in standard equipment at atmospheric pressure to give accurate information on the catalyst decomposition products. The analysis can be operated in an analogous method to *operando* measurements as samples can be drawn at timed intervals, thereby allowing the stability of the catalyst to be monitored over time. This is easily applicable to existing processes, as only the product collector needs to be fitted with a sampler, thus avoiding the need to retrofit the entire plant. *Ex situ* spectroscopy has been reported for reaction monitoring, although this is generally used only to assess the progress of a reaction or for mechanistic studies.[34,35] Catalyst decomposition has been assessed using FTIR, but in a batch process where the decomposition occurred after the substrate was consumed.[36] Here we propose an extension of these techniques to monitor and prevent catalyst degradation during continuous processes.

In a continuous process, when the onset of decomposition is observed, the reaction conditions could be altered to counteract this.[17] For example, the decomposition of triphenylphosphine can be reduced by using lower temperatures, or lower concentrations of alkene.[37] This could preserve the catalyst lifetime, maintain the product selectivity, and reduce costs.

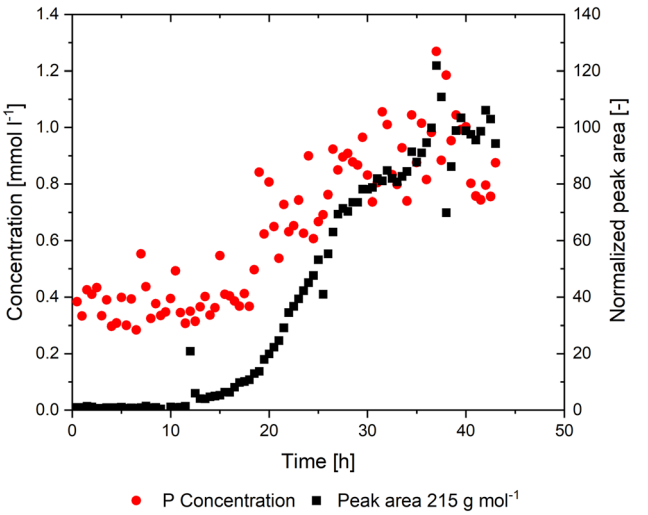

Fig. 7 The concentration of phosphorous in the permeate stream and the peak area of the fragmentation product DPHPO (215 g mol^{-1}), normalized to the initial value. Reaction conditions: T = 125 °C, p = 50 bar, $x_{Rh/P}$ = 1 : 4, $n_{[Rh(acac)(CO)_2]}$ = 0.3 mol%, $n_{Sulfoxantphos}$ = 0.6 mol%, $n_{Cs_2CO_3}$ = 7.5 mol%, $n_{(CO)}$ = $n_{(H_2)}$ = 1 mol h^{-1}, $V_{(Hexene)}$ = 16 mL h^{-1}, $V_{Recycle}$ = 200 mL h^{-1}, $m_{(Circulation)}$ = 60 kg h^{-1}.

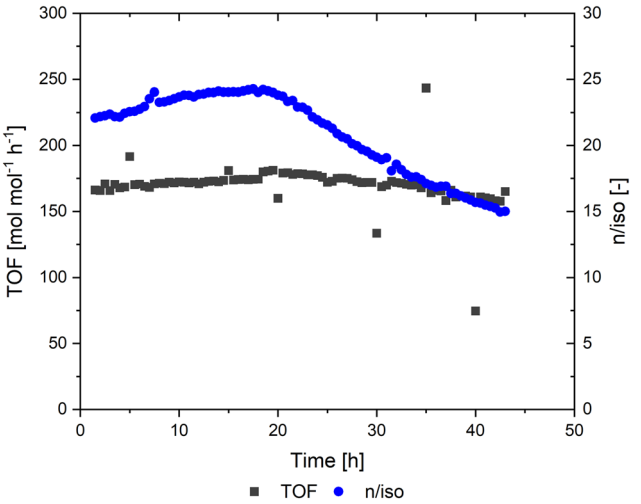

Fig. 8 The TOF and *n*/iso ratio during the continuous reaction. Reaction conditions: T = 125 °C, p = 50 bar, $x_{Rh/P}$ = 1 : 4, $n_{[Rh(acac)(CO)_2]}$ = 0.3 mol%, $n_{Sulfoxantphos}$ = 0.6 mol%, $n_{Cs_2CO_3}$ = 7.5 mol%, $n_{(CO)}$ = $n_{(H_2)}$ = 1 mol h^{-1}, $V_{(Hexene)}$ = 16 mL h^{-1}, $V_{Recycle}$ = 200 mL h^{-1}, $m_{(Circulation)}$ = 60 kg h^{-1}.

Conclusions

We report an alternative to *operando* spectroscopy to monitor the progress of a reaction, and specifically to monitor the stability of a catalyst. Monitoring the contents of the product collector can be performed using standard analytical equipment, whilst still providing useful insights. Using this method, the catalyst stability can be indirectly observed. In our example hydroformylation reaction, a decrease in the *n*/

iso ratio was linked to catalyst deactivation. Furthermore, we were able to use mass spectrometry to determine the pathway of catalyst deactivation, in this case decomposition of the ligand *via* an alkyl/aryl exchange. Performing this analysis during a continuous process would allow the operating conditions to be altered in order to prolong the lifetime of the catalyst, as well as maintaining the initial activity and selectivity, thereby saving time and money by preventing shutdowns in the process.

Methodology section

Reaction setup

The reaction was carried out in a 250 mL windowed reactor (Parr Instruments) equipped with a heating mantle for temperature control. Efficient mixing within the reactor was ensured using a pitched-blade impeller. Precise dosing of the substrate and recycle stream was achieved using HPLC pumps (FluSys) and mass flow controllers (Cori-Flow) from Bronkhorst. The decanter was a custom-built unit with a total volume of 200 mL. Membrane separation was performed using a METcell cross-flow system (Evonik MET Ltd). The active membrane area of the BORSIG oNF-2 membrane was 51 cm^2.

Analytics

GC measurements were performed on a Shimadzu Nexis GC-2030 system equipped with a flame ionization detector (FID) and a CP-Wax 52 CB column (50 m length, 0.25 mm inner diameter). Samples were prepared by diluting 0.1 mL of the product solution with 1 mL of either heptane or isopropanol, respectively. Response factors for all compounds were determined by calibration.

XRF analysis was carried out using a Spectro Xepos C. Each measurement was conducted for 600 s under a helium-air atmosphere at an energy range between 19 eV and 3 keV. For sample preparation, a Prolene film with a thickness of 6 μm was used.

GC/MS measurements were performed using a Shimadzu GC-2010 Plus coupled to a Shimadzu QP2020. Separation was achieved using an RTX-1 column (30 m length, 0.25 mm inner diameter, 0.25 μm film thickness). The injection volume was 0.5 μL with a split ratio of 55 and a linear velocity of 40 cm s^{-1}. The MS interface temperature and injector temperature were both set to 200 °C. Helium was used as the carrier gas.

Chemicals

1-Hexene (97%) and polyethylene glycol (PEG200, average molecular weight = 200 g mol^{-1}) were purchased from Sigma-Aldrich. Cesium carbonate (99.5%) and [Rh(acac)$(CO)_2$] (98.5%) were obtained from Acros Organics. Sodium 4,5-bis(diphenylphosphino)-9,9-dimethyl-9*H*-xanthene-2,7-disulfonate (sulfoxantphos, 99+%) was purchased from Ambeed. Carbon monoxide (99.997%) and hydrogen (99.999%) were supplied by Westfalen AG and Air Liquide, respectively.

All chemicals were degassed prior to use and handled under inert conditions using standard Schlenk techniques or stored in a glovebox.

Conflicts of interest

There are no conflicts to declare.

Data availability

The data supporting this have been included as part of the supplementary information (SI) containing additional graphics, detailed experimental procedures and analytical data.

Supplementary information is available. See DOI: https://doi.org/10.1039/d6red00082g.

Acknowledgements

Open Access funding provided by the Max Planck Society.

References

1 R. H. Crabtree, Deactivation in Homogeneous Transition Metal Catalysis: Causes, Avoidance, and Cure, *Chem. Rev.*, 2015, **115**(1), 127–150.
2 A. J. Martín, S. Mitchell, C. Mondelli, S. Jaydev and J. Pérez-Ramírez, Unifying views on catalyst deactivation, *Nat. Catal.*, 2022, **5**(10), 854–866.
3 S. Zuo, Z.-P. Wu, H. Zhang and X. W. Lou, Operando Monitoring and Deciphering the Structural Evolution in Oxygen Evolution Electrocatalysis, *Adv. Energy Mater.*, 2022, **12**(8), 2103383.
4 D. R. MacFarlane, X. Zhang and M. Kar, Measure and control: molecular management is a key to the Sustainocene!, *Green Chem.*, 2016, **18**(21), 5689–5692.
5 M. Garland, Combining operando spectroscopy with experimental design, signal processing and advanced chemometrics: State-of-the-art and a glimpse of the future, *Catal. Today*, 2010, **155**(3), 266–270.
6 K. Köhnke, N. Wessel, J. Esteban, J. Jin, A. J. Vorholt and W. Leitner, Operando monitoring of mechanisms and deactivation of molecular catalysts, *Green Chem.*, 2022, **24**(5), 1951–1972.
7 T. Hartman, R. G. Geitenbeek, C. S. Wondergem, W. van der Stam and B. M. Weckhuysen, Operando Nanoscale Sensors in Catalysis: All Eyes on Catalyst Particles, *ACS Nano*, 2020, **14**(4), 3725–3735.
8 P. C. J. Kamer, D. Vogt and J. W. Thybaut, *Contemporary Catalysis: Science, Technology, and Applications*, RSC Publishing, Cambridge, 2017.
9 O. Diebolt, P. W. N. M. van Leeuwen and P. C. J. Kamer, Operando Spectroscopy in Catalytic Carbonylation Reactions, *ACS Catal.*, 2012, **2**(11), 2357–2370.
10 M. Garland and C. Li, A Review of BTEM Analysis for Catalytic Studies and a Recent Homogeneous Catalytic Example, *Top. Catal.*, 2009, **52**(10), 1334–1341.

11 C. Kubis, D. Selent, M. Sawall, R. Ludwig, K. Neymeyr and W. Baumann, *et al.*, Exploring Between the Extremes: Conversion-Dependent Kinetics of Phosphite-Modified Hydroformylation Catalysis, *Chem. – Eur. J.*, 2012, **18**(28), 8780–8794.
12 R. Chung and J. E. Hein, The More, The Better: Simultaneous In Situ Reaction Monitoring Provides Rapid Mechanistic and Kinetic Insight, *Top. Catal.*, 2017, **60**(8), 594–608.
13 A. M. R. Hall, P. Dong, A. Codina, J. P. Lowe and U. Hintermair, Kinetics of Asymmetric Transfer Hydrogenation, Catalyst Deactivation, and Inhibition with Noyori Complexes As Revealed by Real-Time High-Resolution FlowNMR Spectroscopy, *ACS Catal.*, 2019, **9**(3), 2079–2090.
14 J. M. Dreimann, E. Kohls, H. F. W. Warmeling, M. Stein, L. F. Guo and M. Garland, *et al.*, In Situ Infrared Spectroscopy as a Tool for Monitoring Molecular Catalyst for Hydroformylation in Continuous Processes, *ACS Catal.*, 2019, **9**(5), 4308–4319.
15 P. W. N. M. van Leeuwen, Decomposition pathways of homogeneous catalysts, *Appl. Catal., A*, 2001, **212**(1), 61–81.
16 N. Wessel, R. S. Medhekar, M. Sonnenberg, H. Stieber, W. Leitner and A. J. Vorholt, Catalyst in Sight: The Use of Benchtop NMR Spectrometers to Maintain the Activity of Pd-PPh3 Catalysts, *ACS Catal.*, 2024, **14**(14), 10679–10688.
17 J. T. Vossen, F. Patzina, W. Leitner and A. J. Vorholt, Studying the Recycling and Deactivation of Rh/Biphephos Complexes in the Isomerization–Hydroformylation Tandem Reaction, *ACS Sustainable Chem. Eng.*, 2024, **12**(28), 10665–10677.
18 T. A. Fassbach, J.-M. Ji, A. J. Vorholt and W. Leitner, Recycling of Homogeneous Catalysts–Basic Principles, Industrial Practice, and Guidelines for Experiments and Evaluation, *ACS Catal.*, 2024, **14**(9), 7289–7298.
19 S. Störtte, L. Steinwachs, R. S. Medhekar, R. Novemen and A. J. Vorholt, Systematic Comparison of Homogeneous Catalyst Recycling Strategies: Organic Solvent Nanofiltration vs. Liquid-Liquid-Multiphase, *Chem. – Eur. J.*, 2025, e03075.
20 J. Dreimann, P. Lutze, M. Zagajewski, A. Behr, A. Górak and A. J. Vorholt, Highly integrated reactor–separator systems for the recycling of homogeneous catalysts, *Chem. Eng. Process.: Process Intesif.*, 2016, **99**, 124–131.
21 J. M. Dreimann, F. Hoffmann, M. Skiborowski, A. Behr and A. J. Vorholt, Merging Thermomorphic Solvent Systems and Organic Solvent Nanofiltration for Hybrid Catalyst Recovery in a Hydroformylation Process, *Ind. Eng. Chem. Res.*, 2017, **56**(5), 1354–1359.
22 T. Gaide, J. M. Dreimann, A. Behr and A. J. Vorholt, Overcoming Phase-Transfer Limitations in the Conversion of Lipophilic Oleo Compounds in Aqueous Media—A Thermomorphic Approach, *Angew. Chem., Int. Ed.*, 2016, **55**(8), 2924–2928.
23 M. Strohmann, J. T. Vossen, A. J. Vorholt and W. Leitner, Recycling of two molecular catalysts in the hydroformylation/aldol condensation tandem reaction using one multiphase system, *Green Chem.*, 2020, **22**(23), 8444–8451.
24 M. Zagajewski, J. Dreimann, M. Thönes and A. Behr, Rhodium catalyzed hydroformylation of 1-dodecene using an advanced solvent system: Towards highly efficient catalyst recycling, *Chem. Eng. Process.: Process Intesif.*, 2016, **99**, 115–123.
25 Organic Solvent Nanofiltration [available from: https://www.osn-membranes.com/what-is-osn/borsig-membranes.
26 S. Van Buggenhout, G. Ignacz, S. Caspers, R. Dhondt, M. Lenaerts and N. Lenaerts, *et al.*, Open and FAIR data for nanofiltration in organic media: A unified approach, *J. Membr. Sci.*, 2025, **713**, 123356.
27 H. Zhang, Q. He, J. Luo, Y. Wan and S. B. Darling, Sharpening Nanofiltration: Strategies for Enhanced Membrane Selectivity, *ACS Appl. Mater. Interfaces*, 2020, **12**(36), 39948–39966.
28 P. Marchetti, M. F. Jimenez Solomon, G. Szekely and A. G. Livingston, Molecular Separation with Organic Solvent Nanofiltration: A Critical Review, *Chem. Rev.*, 2014, **114**(21), 10735–10806.
29 P. Vandezande, L. E. M. Gevers and I. F. J. Vankelecom, Solvent resistant nanofiltration: separating on a molecular level, *Chem. Soc. Rev.*, 2008, **37**(2), 365–405.
30 J. Geens, A. Hillen, B. Bettens, B. Van der Bruggen and C. Vandecasteele, Solute transport in non-aqueous nanofiltration: effect of membrane material, *J. Chem. Technol. Biotechnol.*, 2005, **80**(12), 1371–1377.
31 J. T. Scarpello, D. Nair, L. M. Freitas dos Santos, L. S. White and A. G. Livingston, The separation of homogeneous organometallic catalysts using solvent resistant nanofiltration, *J. Membr. Sci.*, 2002, **203**(1), 71–85.
32 A. Kütt, S. Selberg, I. Kaljurand, S. Tshepelevitsh, A. Heering and A. Darnell, *et al.*, pKa values in organic chemistry – Making maximum use of the available data, *Tetrahedron Lett.*, 2018, **59**, 3738–3748.
33 A. G. Abatjoglou, E. Billig and D. R. Bryant, Mechanism of rhodium-promoted triphenylphosphine reactions in hydroformylation processes, *Organometallics*, 1984, **3**(6), 923–926.
34 A. Ray, T. Bristow, C. Whitmore and J. Mosely, On-line reaction monitoring by mass spectrometry, modern approaches for the analysis of chemical reactions, *Mass Spectrom. Rev.*, 2018, **37**(4), 565–579.
35 C. Rougeot, H. Situ, B. H. Cao, V. Vlachos and J. E. Hein, Automated reaction progress monitoring of heterogeneous reactions: crystallization-induced stereoselectivity in amine-catalyzed aldol reactions, *React. Chem. Eng.*, 2017, **2**(2), 226–231.
36 R. Theron, Y. Wu, L. P. E. Yunker, A. V. Hesketh, I. Pernik and A. S. Weller, *et al.*, Simultaneous Orthogonal Methods for the Real-Time Analysis of Catalytic Reactions, *ACS Catal.*, 2016, **6**(10), 6911–6917.
37 R. M. Deshpande, S. S. Divekar, R. V. Gholap and R. V. Chaudhari, Deactivation of homogeneous HRh(CO)(PPh3)3 catalyst in hydroformylation of 1-hexene, *J. Mol. Catal.*, 1991, **67**(3), 333–338.